Special Technique for Growing Tl_4S_3, Anisotropy of Electrical Conduction and Photophysical Properties

H. A. Elshaikh, I. M. Ashraf, and A. M. Badr*

Physics Department, Faculty of Science (Aswan), South Valley University, Egypt

Received: August 26, 2003; In Final Form: June 3, 2004

Single crystals of Tl_4S_3 were prepared by using a special local technique and the obtained crystals were analyzed by X-ray diffraction. The electrical properties (electrical conductivity and Hall effect) and steady-state photoconductivity for the resultant crystals were elucidated in this work. The electrical measurements extend from 170 to 430 K. $\sigma_\perp = 4.263 \times 10^{-6}$ $(\Omega\ cm)^{-1}$ when current flow direction makes a right angle to the cleavage plane of the crystals, but $\sigma_{||} = 1.034 \times 10^{-6}$ $(\Omega\ cm)^{-1}$ when the current flow is parallel to the cleavage plane. The width of the band gap is calculated using the electrical conductivity and Hall Effect measurements, and the values are discussed. The anisotropy of the electrical conductivity ($\sigma_\perp/\sigma_{||}$) in the Tl_4S_3 single crystals was also studied in this work. Finally, the photosensitivity was calculated for different levels of illumination. The results of the photoconductivity study showed that the recombination process in Tl_4S_3 single crystals is monomolecular.

1. Introduction

Tl_4S_3 single crystals are highly anisotropic compounds of the III−VI semiconductor family. This family has much importance in the field of both fundamental research and technical applications because of its structure, optical, electronic, and photoelectronic properties. An investigation of optical and electrical properties of the highly anisotropic compounds revealed that they are promising semiconductors for applications in photoelectric devices in the visible region.[1] Layered crystals were largely used to test some of the most advanced techniques in modern photoemission study.[2] The interest in these materials is stimulated not only by their fundamental properties but also by possible practical applications.[3] Recently, ternary thallium chalcogenides received a great deal of attention due to their optical and electrical properties in view of possible optoelectronic device applications.[4−7]

TlS and Tl_4S_3 are double sulfides: $Tl^I[Tl^{III}S_2]$ and $Tl^I{}_3[Tl^{III}S_3]$, respectively; whereas TlS_2, Tl_2S_5, Tl_2S_9, etc., may be considered as polysulfides Tl_xSS_n (for example, Tl_2SS_8 with elemental composition: Tl_2S_9).[8] Thin film coatings of Tl_4S_3 or Tl_2S of 100−750 nm in thickness have been deposited from a mixture of citratothallium complex and thiourea solutions at 35 or 50 °C by chemical bath deposition on glass substrates coated with a thin ZnS film.[9] The resultant material of the film is Tl_4S_3. Estrella et al. also showed that upon heating in a nitrogen atmosphere at 300 °C, all the films, irrespective of the initial composition, convert to crystalline Tl_2S. The crystalline structure of thin films of thickness of 500 nm deposited at room temperature on clean glass slides from baths containing 20 mL of 0.2 M thallium nitrate, 30 mL of 14 M ammonia, and 4 mL of 1 M thiourea has been determined to be of TlS.[10] Thin films obtained from a bath mixture containing thallium sulfate, triethanolamine, ammonia, and sodium selenosulfate[11] deposited at 30 °C on glass slides, as well as those obtained from baths constituted from thallium acetate, sodium selenosulfate, sodium hydroxide, and hydrazine,[12] have been confirmed to be TlSe. These compositions result from bonding of the double sulfide $Tl^I[Tl^{III}S_2]$ or double selenide $Tl^I[Tl^{III}Se_2]$, which requires the generation of Tl^{III} species, in an abundance equal to that of Tl^I in the bath. Chalcogenide semiconducting thin films having an optical gap in the range 1.5−2.5 eV have been receiving considerable attention in recent years because of the possibility of their utilization in fabrication of solar cells.[13]

In the present work, a special local technique is used for preparing thallium Tl_4S_3 single crystals. The aim of the work is to elucidate the preparation process, electrical properties, and photophysical properties for the obtained crystals.

2. Sample Preparation and Characterization

Tl_4S_3 single crystals were prepared by a special local technique in the Solid State Laboratory, Physics Department, Faculty of Science, South Valley University, Aswan, Egypt. This technique is an apparatus consisting of two parts. The first part is a Lenton Thermal Design (LTD) in which heating is via silicon carbide rod elements that are mounted parallel to the ceramic work-tube of this design. The outer case is manufactured from a zinc-coated steel sheet and finished with a tough. The outer mesh cover allows natural air cooling for safety. If the ends of the work-tube of this design are plugged to prevent excessive heat loss, the temperature variation within the uniform zone (the area in the work-tube in which the compound should be placed) is ±5 °C for single zone control, whereas the uniformity is ±2 °C for multi-zone control (the usual configuration is three-zone control). The LTD used for preparing Tl_4S_3 single crystals is a three-zone control, where for such a zone there is a temperature controller (eurotherm 91e-type) with dual four-digit display for simultaneous viewing of the setpoint and measured values. These temperature controllers include a single ramp to temperature. The second part is a wood block, which was shaped in a triangle form. If the triangle is used as a base for the first part (LTD), the work-tube of this design makes a 45° angle with the horizontal. The silica tube containing the Tl_4S_3 compound was covered by a mesh of nickel chrome and held between two highly thermal insulator disks. Thereafter, this work-group was placed in the determined length inside the

10.1021/jp031035z CCC: $27.50
Published on Web 07/10/2004

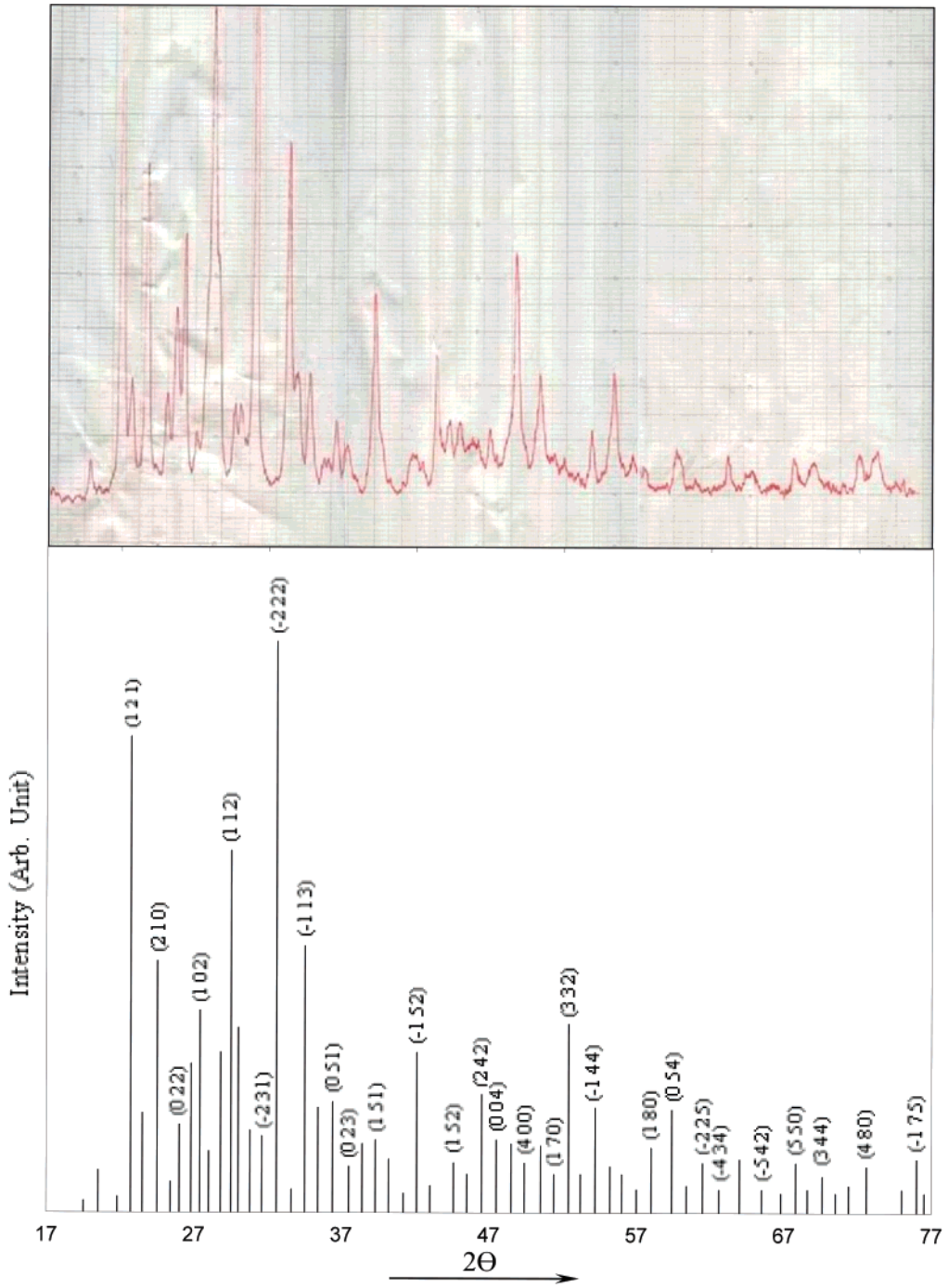

Figure 1. The XRD diffraction pattern of the obtained Tl_4S_3 single crystals.

work-tube, making the same angle with the horizontal (45°). The work-group prevents cold air from being propagated from the external environment into the work-group, leading to a desired homogeneity of heat inside the work-group. Single crystals of Tl_4S_3 were prepared from pure (5N) elements (Aldrich Mark) in an evacuated silica tube (10^{-6} Torr) of 1.5 cm in diameter and 20 cm in length. The charge elements are weighted to be 3.4061 g of thallium and 0.4008 g of sulfur by using an electronic balance (Sartorius-Mark) with a sensitivity of 10^{-4} g. The silica tube containing Tl_4S_3 was placed in the center of the uniform zone within the work-tube. The temperature profile inside the uniform zone can be controlled by the three digital temperature controllers of the LTD. The temperature in the uniform zone of the work-tube was adjusted, by using these digital controllers, to be higher than the melting point of Tl_4S_3. This condition was maintained for 24 h, during which the melt was shaken several times in order to accelerate the diffusion of the constituents through each other, leading to the melt homogenization. Thereafter, the three digital temperature controllers were used to supply a narrow temperature gradient along the uniform zone in which the silica tube containing the compound was placed. In the final step, the temperature profile affected on the compound is still higher than its melting point. Then the crystallization process was achieved by cooling the melt slowly with rate at a rate of 3 C°/h. The crystal structure of obtained Tl_4S_3 crystals was identified using XRD analysis at room temperature. Diffraction of the obtained crystals is compared with the index of the American Society for Testing Materials (ASTM) cards. In this way, the crystal natures of the obtained crystals have been confirmed by comparing the values

TABLE 1: The Crystallographic Data "Obtained and Standard" for Tl_4S_3 Crystals

		d (Å)				*d* (Å)	
h k l	I/I_o	obtained	standard	*h k l*	I/I_o	obtained	standard
(1 2 1)	5	3.91	3.89	(2 4 1)	18	2.25	2.249
(0 3 1)	40	3.79	3.78	(−1 5 2)	17	2.15	2.151
(2 1 0)	79	3.63	3.61	(1 5 2)	18	2.01	2.007
(0 2 2)	100	3.34	3.32	(2 4 2)	4	1.95	1.945
(2 2 0)	64	3.26	3.25	(0 0 4)	9	1.94	1.932
(1 0 2)	30	3.16	3.15	(4 0 0)	22	1.88	1.881
(−2 0 2)	75	3.08	3.08	(1 7 0)	24	1.81	1.805
(1 1 2)	52	3.04	3.06	(3 3 2)	2	1.74	1.748
(0 4 1)	57	3.00	3.00	(−1 4 4)	18	1.69	1.696
(−1 4 1)	54	2.88	2.877	(1 8 0)	23	1.59	1.589
(−2 3 1)	34	2.84	2.836	(0 5 4)	7	1.55	1.551
(−2 2 2)	4	2.76	2.784	(−2 2 5)	1	1.52	1.522
(−1 1 3)	9	2.57	2.582	(−4 3 4)	2	1.45	1.451
(2 3 1)	50	2.53	2.528	(−5 4 2)	2	1.38	1.383
(0 5 1)	34	2.46	2.466	(5 5 0)	3	1.3	1.302
(0 2 3)	15	2.39	2.396	(3 4 4)	5	1.27	1.273
(3 2 0)	16	2.34	2.34	(4 8 0)	14	1.23	1.231
(1 5 1)	16	2.3	2.294	(−1 7 5)	6	1.21	1.208

of the interplanar distance (*d*) calculated from the peaks and those recorded in the ASTM card[14] (see Figure 1 and Table 1). This comparison showed that the Tl_4S_3 obtained is in single-crystal form with monoclinic symmetry, space group $P21/c$, and lattice parameters $a = 7.7373$ Å, $b = 13.0120$ Å, $c = 7.9499$ Å, and $Z = 4$. It is evident that the crystals have a high degree of crystallinity, indicating that the preparation technique is fairly reliable and satisfactory.

3. Sample Contact and Connections

The bulk sample, which was used in measurements, was prepared by splitting the crystal along the cleavage plane, and hence the resultant surface was mirrorlike without any mechanical treatment. Samples used in measurements were formed in suitable shapes. Then the sample under study was mounted on the coldfinger inside a cryostat (Oxford DN1704-type), which was evacuated to about 10^{-4} Torr. The temperature inside the cryostat was controlled by a digital temperature controller (Oxford ITC601-type). The contacts between the samples and the metal electrodes were made by using silver paste. The electrical contacts have been tested to analyze their $I-V$ characteristics and are found to be ohmic in the whole investigated range of the applied voltage. The electrical measurements were made with the aid of an electrometer (Keithly 610-type). An Oxford electromagnet of type N177 with its suitable regulated and stabilized power supply of type SC7 was used as a source of the external magnetic field for Hall Effect measurements. For measuring the magnetic field intensity and its homogeneity, calibration was done with the aid of an Oxford Hall magnetometer, model 5200. The Hall voltage was measured by using a potentiometer of type UJ33E with a sensitivity up to 10^{-6}. In photoconductivity measurements, excitation was done by a tungsten lamp of 1000 W. The incident light was focused by using an optical system consisting of two convex lenses, which enables homogeneous illumination to be obtained. This optical system allows accurate measurements of the light intensity at the surface of the specimen and keeps it far from the lamp, avoiding the lamp's heat.

4. Electrical Properties

4.1. Electrical Conductivity. For electrical conductivity measurements, a sample of Tl_4S_3 single crystals was prepared by cleavage parallel in direction to the layers of these crystals. The resultant platelike sample was treated as having a rectangular shape with dimensions $1.2 \times 2.5 \times 8$ mm. The electrical conductivity (σ) was measured in two cases: one of them is that σ was measured when the current flow direction is perpendicular to the cleavage plane ($\sigma_\perp$), and the other is when the current flow is parallel to the cleavage plane ($\sigma_\parallel$). At room temperature, it was found that $\sigma_\perp = 4.263\ (\text{cm})^{-1}$. The temperature dependence of the electrical conductivities ($\sigma_\parallel$ and $\sigma_\perp$) for a Tl_4S_3 single crystal in the whole investigated temperature range (from 170 to 430 K) is presented in Figure 2. It is clear from this figure that the Arrhenius behavior is observed in three linear regions for the whole investigated range of temperature; moreover, $\sigma_\perp$ differs from $\sigma_\parallel$, which suggests anisotropy of the electrical conductivity in Tl_4S_3 single crystals. The first region (I) corresponds to low temperatures, where the electrical conductivity in this range could be attributed to the extrinsic transitions; the second region (II) may be considered as the transition region from conduction via extrinsic transitions to that via intrinsic transitions; the third region (III) corresponds to high temperatures, where the intrinsic transitions are responsible for the current flow (where there is no effect of impurities on $\sigma_\parallel$ or $\sigma_\perp$). Figure 2 also suggests that the electrical conductivities of Tl_4S_3 single crystals slowly increase in the extrinsic region with increase in temperature satisfying the relation:

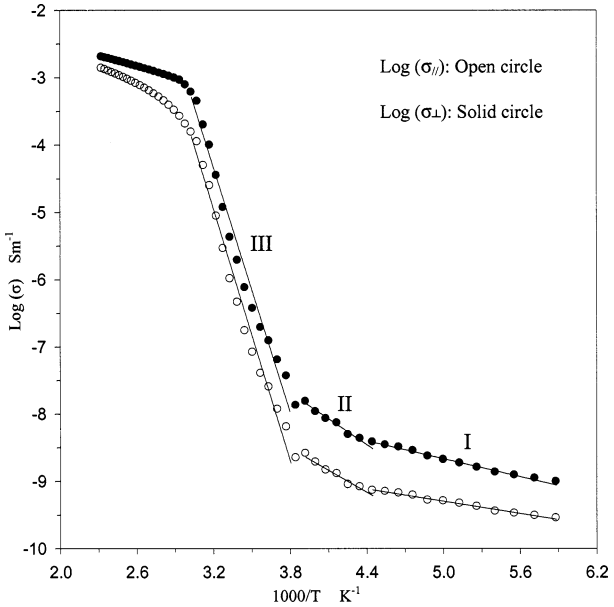

Figure 2. Reciprocal temperature dependence of electrical conductivity in Tl_4S_3 single crystals.

$$\sigma = \sigma_o \exp\left[-\frac{E_a}{2kT}\right] \quad (1)$$

where σ_o is the preexponential factor, and E_a is the activation energy. The extrinsic region (I) starts from 170 to 225 K with activation energies of 0.076 eV for $\sigma_\perp$ and 0.052 eV for $\sigma_\parallel$. The temperature dependence of electrical conductivity in the transition region (the range of temperature lying between the extrinsic behavior and intrinsic behavior regions) is greater than that in the extrinsic region. This region starts from 225 to 255 K with activation energies of 0.22 eV for $\sigma_\perp$ and 0.19 eV for $\sigma_\parallel$. The electrical conductivity of Tl_4S_3 single crystals rapidly increases in the intrinsic region with an increase in temperature (Figure 2) following the relation:

$$\sigma = \sigma_o \exp\left[-\frac{E_g}{2kT}\right] \quad (2)$$

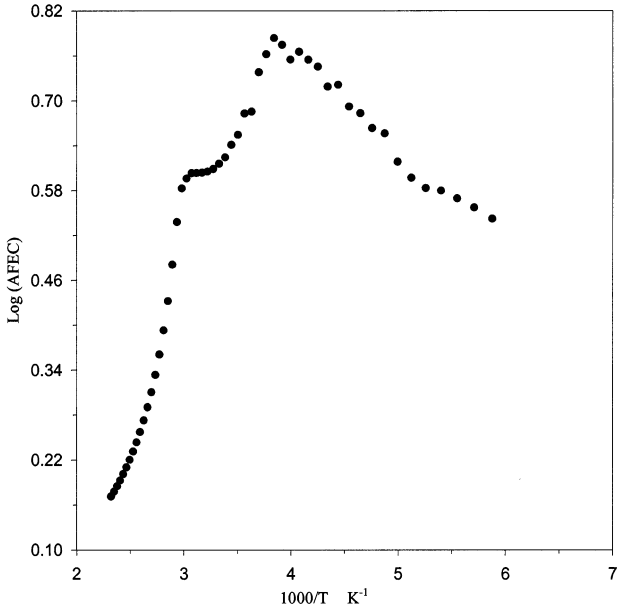

Figure 3. Dependence of the anisotropic factor of electrical conductivity on temperature for Tl_4S_3 single crystals.

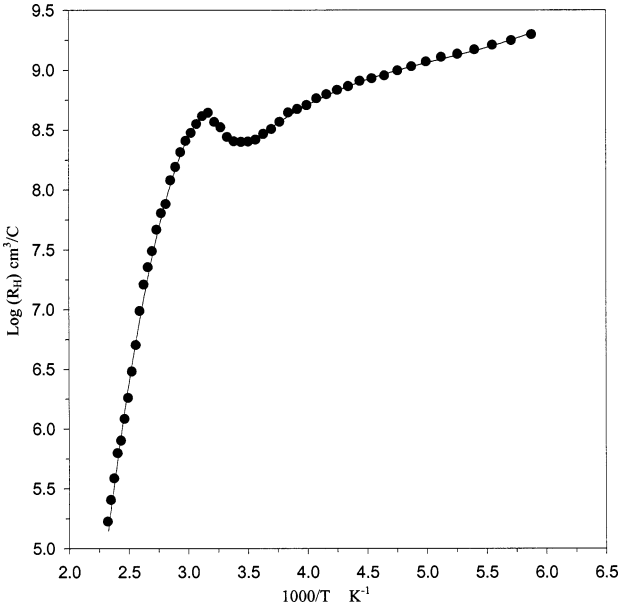

Figure 4. Temperature dependence of the Hall coefficient for TlS single crystals.

This region starts from 260 to 330 K with a band gap of widths $E_g = 1.05$ eV for $\sigma_\perp$ and $E_{g||} = 1.08$ eV for $\sigma_{||}$. Below 170 K the electrical conductivity is almost constant, indicating the freezing of charge carriers.

A previous work reported by Busch et al.[15] showed that the anisotropic factor of electrical conductivity ($\sigma_\perp/\sigma_{||}$) is independent of temperature, but in another previous investigation obtained by Schmid et al.,[16] it was observed that [$(\sigma_\perp/\sigma_{||}) \propto \exp(E_g/kT)$]. In the present work, it is clear that the temperature dependence of the anisotropic factor of electrical conductivity (AFEC) in Tl_4S_3 single crystals is in agreement with the later investigation[16] and is governed by the relation given above (see Figure 3). This figure illustrates the variation of anisotropic factor ($\sigma_\perp/\sigma_{||}$) with temperature in the same investigated range (i.e., 170 to 430 K) with which the electrical conductivity measurements were carried out. The figure suggests that the anisotropic factor of electrical conductivity depends strongly on temperature in the range 260 to 430 K and its temperature dependence is greater than that in the temperature range 77 to 260 K. Also, Figure 3 suggests that $\sigma_\perp < \sigma_{||}$ in the whole investigated temperature range (from 170 to 430 K). Therefore, the electrical conductivity of Tl_4S_3 single crystals is highly anisotropic, which could be attributed partly or wholly to the interlayer macroscopic defects or planes of precipitates, where the low values of $\sigma_{||}$ or $\sigma_\perp$ are due to the presence of the so-called "two-dimensional defects" located between the layers that govern the carrier motion across the layers.[17,18,19]

4.2. Hall Effect. The electrical conductivity measurements were extended to elucidate the temperature dependence of the Hall coefficient for Tl_4S_3 single crystals and to determine important physical parameters. Also, the scattering mechanism for the charge carriers was elucidated and discussed in this section. In this experiment the current passes through the specimen in the direction parallel to the cleavage plane, where the external magnetic field is oriented perpendicular to the given plane. The specimen dimensions used in this experiment are the same as those used in the electrical conductivity measurements. The temperature range investigated with which the Hall Effect measurements were carried out is also the same for the electrical conductivity measurements. The temperature dependence of the Hall coefficient for Tl_4S_3 single crystals is illustrated in Figure 4; this figure suggests that at room temperature the Hall coefficient "R_H" has a value of about 273 777 746.66 cm^3/C and the hole concentration "p" was calculated to be 2.28×10^{11} cm^{-3}. A positive sign of R_H through all the temperature range investigated is indicative of holes providing the major contribution to the electrical conductivity (i.e., the Tl_4S_3 single crystal is a p-type semiconductor); R_H varies linearly in three regions of the temperature range investigated (extrinsic, transition, and intrinsic regions). Figure 4 also suggests that the Tl_4S_3 single crystal exhibits a considerable decline of R_H in the temperature region referring to low temperature, but it falls rapidly in the temperature region corresponding to the transition region with a higher slope than it has for the low-temperature region. Through the high investigated temperature referring to the intrinsic region, R_H falls more rapidly with the highest slope of those for the above given regions.

The relation between $R_H T^{3/2}$ and $1000/T$ for Tl_4S_3 single crystals is depicted in Figure 5, which suggests that $R_H T^{3/2}$ increases linearly with an increase in temperature; this linear increase is observed in three regions of the temperature range investigated. With the aid of this figure, we can compare and discuss the data calculated from this figure with that reported in the previous section or confirm the latter: The intrinsic region is observed in the temperature interval 360 to 430 K from which the forbidden gap width (E_g) is calculated to be about 0.98 eV (the values of E_g calculated from electrical conductivity measurements are $E_g = 1.05$ eV and $E_{g||} = 1.08$ eV). The activation energy corresponding to the transition region has a value of about 0.102 eV (activation energy has a value of about 0.22 eV for $\sigma_\perp$-measurements and 0.19 eV for $\sigma_{||}$-measurements). But the activation energy referring to the extrinsic region, which is observed in the temperature interval from 170 to 250 K, is calculated to be 0.029 eV (0.076 eV for $\sigma_\perp$-measurements and 0.052 eV for $\sigma_{||}$-measurements).

Bube[20] reported conclusions about the effect of scattering on the mobility of charge carriers and asserted that the mobility in materials with predominantly covalent bonding will usually be higher than the mobility in materials with predominantly ionic bonding. The temperature dependence of the mobility as the result only of interaction between charge carriers and acoustical

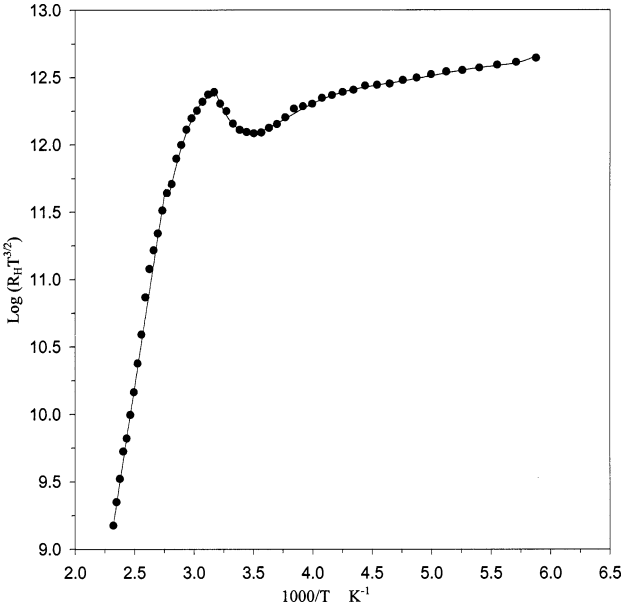

Figure 5. Plot of $R_HT^{3/2}$ versus 1000/T for TlS single crystals.

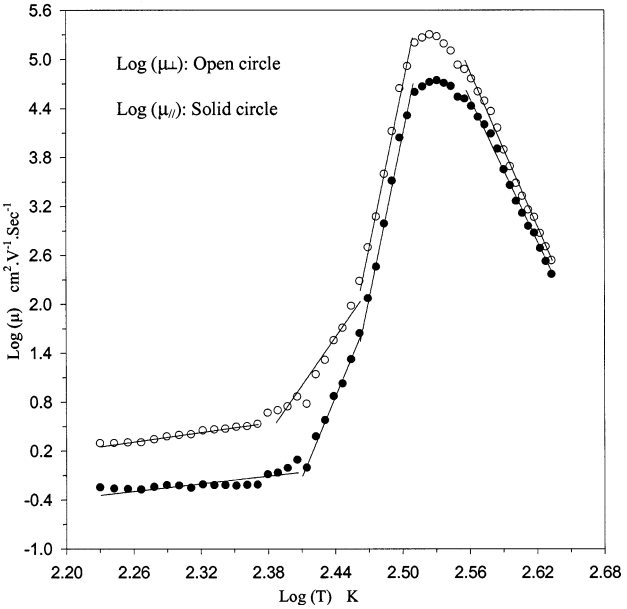

Figure 6. Temperature dependence of the Hall mobility for TlS single crystals.

vibrations in nonionic crystals has been shown by Bardeen and Shockley[21] for spherical equal-energy surfaces to have the form

$$\mu \propto T^{-3/2} \tag{3}$$

In the present work the temperature dependence of the Hall mobility for Tl_4S_3 single crystals is illustrated in Figure 6, which describes four linear behaviors of the Hall mobility with variation of temperature; this figure shows that there is a linear dependence of log μ on log T in the low-temperature range 170 to 235 K with a slope of 1.9 ($\mu \alpha T^{1.9}$) for $\mu_\perp$, as well as a linear dependence of log μ on log T in the low-temperature range 170 to 255 K with a slope of 1.56 ($\mu \alpha T^{1.56}$) for $\mu_{||}$. The exponent of the above relation suggests that the temperature dependence of the Hall mobility in the mentioned low-temperature intervals may be considered as a result only of interaction between charge carriers and acoustical lattice vibrations.[21]

But in the high-temperature regions there are three linear dependences of log μ on log T for both the investigated directions of current: 240 to 290 K, 290 to 325 K, and 355 to 430 K for both $\mu_\perp$ and $\mu_{||}$. For all the given high intervals of temperatures, the Hall mobility shows considerable deviations from the exponent included in eq 3. To our knowledge, there are no reported data in the literature on the electrical properties of Tl_4S_3 single crystals in the high-temperature region. An anomalous behavior of the temperature dependence of Hall mobility similar to what has been observed in the present work has also been reported by Nagat[22] in highly resistive thallium monosulfide single crystals, and it is proposed to be due to a change in transport mechanism between localized states either within the energy gap or in the regions close to the band edges. On the other hand, anomalous behavior of the Hall data for HgCdTe layers was reported in the literature and a model has been proposed in which a narrow band gap material having inclusions of the opposite conduction type was considered.[23] The model was applied to n-type HgCdTe by assuming it to contain random distributions of macroscopic domains of different (or the same) conduction type and doping level. The domains considered were microscopically large so that inhomogeneity cannot be treated by scattering mechanisms. The measured Hall coefficient was interpreted by taking the volume fraction and the Hall coefficient of the p-type domain into consideration. The observed anomalous temperature dependence of mobility at high temperature in the present Tl_4S_3 crystals together with its order-of-magnitude lower value as compared to earlier results[24] may be due to different features of the microstructure as the formation of p-type domains during the crystal growth stage.[23] This interpretation also supports an explanation given by Nagat[22] since the parasitic phases in the form of inclusions are expected to result in new localized states.

For our specimen of Tl_4S_3 single crystals, the $\mu-T$ relation can be described in the high-temperature regions as follows. According to eq 3, the temperature dependence of the mobility in all the mentioned high-temperature intervals is a result not only of interaction between charge carriers and acoustical vibrations, but also another scattering mechanism. One attempt to explain the above-mentioned deviations from eq 3 involves taking account of a contribution to the scattering from optical vibration.[20,25] Hence the observed mobility in Tl_4S_3 single crystals may be considered as the result of the mobility determined by a contribution to scattering from acoustical vibrations and the mobility determined by a contribution to scattering from optical vibrations. As results of Hall effect measurements, at room-temperature R_H, p, $\mu_\perp$, and $\mu_{||}$ are calculated to be 273 777 746.66 cm^3/C, 2.28 $\times$ 10^{11} cm^{-3}, 1167.15 cm^2 V^{-1} s^{-1}, and 283.16 cm^2 V^{-1} s^{-1}, respectively.

5. Steady-State Photoconductivity

The total current (dark current + photocurrent) was measured at room temperature for different levels of illumination: 0.6 F, 1.2 F, 1.8 F, 2.4 F, 3 F, 3.6 F and 4.2 F, where F = 1000 Lux. The photocurrent was obtained by subtracting the dark current from the total current. The dependences of the dark current and photocurrent on the applied voltage for Tl_4S_3 single crystals are illustrated in Figure 7. This figure shows that the dark current as well as the photocurrent linearly increases with the increase in voltage in the whole investigated range of the applied voltage (i.e., 4−28 V). The photosensitivity determined for Tl_4S_3 single crystals using the relation $S = [\sigma_{ph}/\sigma_d]$ for different levels of illumination was found as 0.046, 0.091, 0.14, 0.16, 0.23, 0.26, and 0.31 for light intensities 0.6 F, 1.2 F, 1.8 F, 2.4 F, 3 F, 3.6 F, and 4.2 F, respectively. The photocurrent was plotted as a function of the light intensity (see Figure 8). It is clear from

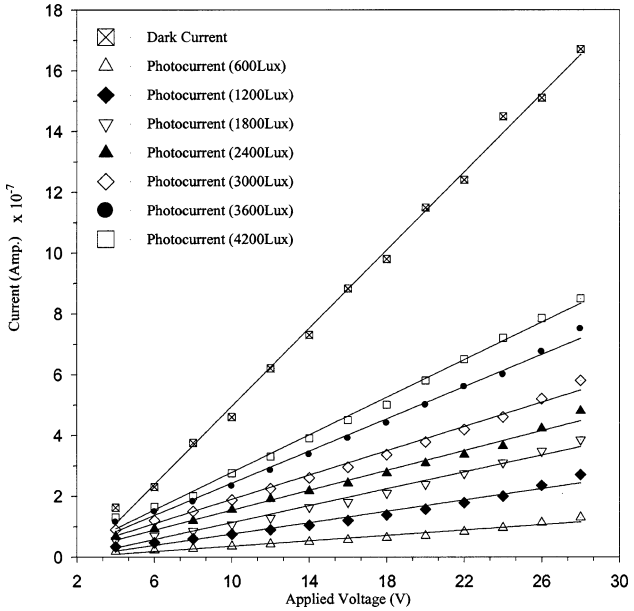

Figure 7. Dark current and photocurrent as functions of the applied voltage at different levels of illumination in Tl_4S_3 single crystals.

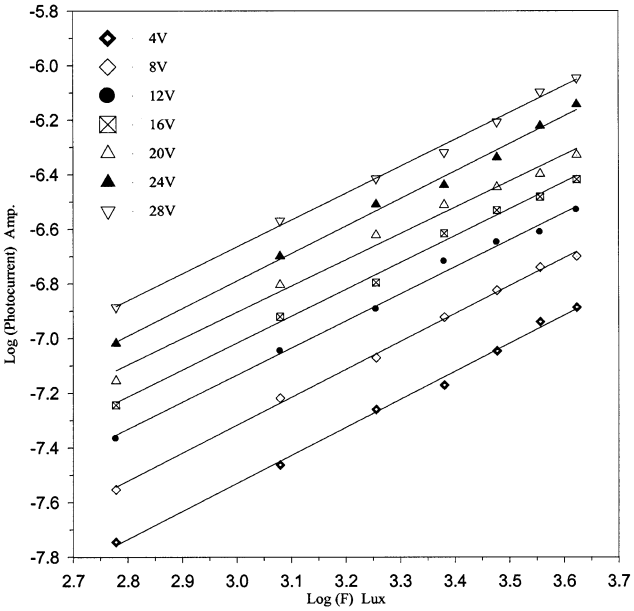

Figure 8. Light intensity dependence of the photocurrent for Tl_4S_3 single crystals.

this figure that the photocurrent linearly increases with the increase in light intensity, which could be due to the generation of a greater number of free charge carriers. So the relation between the photocurrent and light intensity obeys the power law

$$I_{ph} \propto F^{\gamma} \tag{4}$$

where γ is a constant, and its value determines whether the recombination process is monomolecular or bimolecular. For $\gamma = 0.5$, the recombination process is bimolecular (square root), but for $\gamma = 1$ it is a monomolecular (linear) process. If the value of γ lies between 0.5 and 1 (sublinear), it suggests that there is a continuous distribution of impurity states.[26] In the present study, it is found that the value of γ lies between 0.96 and 1.02. This indicates that the recombination process in Tl_4S_3 single crystals is a monomolecular process.

6. Conclusion

Due to difficulties in preparing Tl_4S_3 in single-crystal form, a special local technique was used for growing this compound. The resultant crystals were analyzed using XRD, which showed that the obtained Tl_4S_3 is in single-crystal form with monoclinic symmetry, space group: $P21/c$ and lattice parameters: $a = 7.7373$ Å, $b = 13.0120$ Å, $c = 7.9499$ Å, and $Z = 4$. The electrical conduction was elucidated for the resultant crystals; at room temperature it was found that $\sigma_{\perp} = 4.263 \times 10^{-6}$ and $\sigma_{\parallel} = 1.034 \times 10^{-6}$ $(\Omega\ \mathrm{cm})^{-1}$. Plotting $(\sigma_{\perp}/\sigma_{\parallel})$ versus temperature, it was observed that the electrical conductivity in Tl_4S_3 single crystals is highly anisotropic, especially in the low-temperature regions. Hall effect measurements confirm the data obtained in the electrical conductivity measurements and describe a new discussion for the $\mu - T$ relation for Tl_4S_3 single crystals. At room temperature, R_H, p, $\mu_{\perp}$, and $\mu_{\parallel}$ are calculated to be 273 777 746.66 cm^3/C, 2.28×10^{11} cm^{-3}, 1167.15 $cm^2\ V^{-1}\ s^{-1}$, and 283.16 $cm^2\ V^{-1}\ s^{-1}$, respectively. Photoconductivity measurements were studied in the applied voltage range 4 to 28 V for different levels of illumination from 0.6 F to 4.2 F (F = 1000 Lux). The results showed that the photosensitivity of Tl_4S_3 single crystals varies from 0.046 to 0.31 for the variation in the light intensity from 0.6 F to 4.2 F. It was also found that the recombination process in Tl_4S_3 single crystals is monomolecular.

Acknowledgment. The authors are much indebted to Prof. Dr. A. E. Belal (Physics Department, Faculty of Science "Aswan", South Valley University, Egypt) for his help and encouragement.

References and Notes

(1) Kyazymzade, A.; Mekhtieva, N.; Akhmedov, A. *Sov. Phys. Semicond.* **1992**, *25*, 90.
(2) Ashraf, I. M.; Abdel-Rahman, M. M.; Badr, A. M. *J. Phys. D: Appl. Phys.* **2003**, *36*, 109−113.
(3) Youssef, S. B. *Physica A* **1995**, *215*, 176−180.
(4) Yee, K. A.; Albright, A. *J. Am. Chem. Soc.* **1991**, *113*, 6474.
(5) Hanias, M. P.; Anagnostopoulos, A. N.; Kambas, K.; Spyridelis, J. *Mater. Res. Bull.* **1992**, *27*, 25.
(6) Kalkan, N.; Kalomiros, J. A.; Hanias, M.; Anagnostopoulos, A. N. *Solid State Commun.* **1996**, *99*, 375.
(7) Kalomiros, J. A.; Kalkan, N.; Hanias, M.; Anagnostopoulos, A. N.; Kambas, K. *Solid State Commun.* **1995**, *96*, 601.
(8) Lee, A. G. In *The chemistry of thallium*; Monograph 14 in the Series Topics in Inorganic Chemistry; Robinson, P. L., Ed.; Elsevier: Amsterdam, 1971.
(9) Estrella, V.; Nair, M. T. S.; Nair, P. K. *Thin Solid Films* **2002**, *414*, 289−295.
(10) Mondal, A.; Pramanik, P. *Thin Solid Films* **1983**, *110*, 65.
(11) Bhattacharya, R. N.; Pramanik, P. *Bull. Mater. Sci.* **1981**, *3*, 403.
(12) Mangalam, M. J.; Nagaraja Rao, K.; Rangarajan, N.; Siddiqi, M. I. A.; Suryanarayana, C. V. *Jpn. J. Appl. Phys.* **1969**, *8*, 1258.
(13) Patil, A. R.; Patil, V. N.; Anuse, M. A.; Bhosale, P. N.; Deshmukh, L. P. *Thin Solid Films* **2002**, *414*, 155−162.
(14) Berger, R. Uppsala Universitet, Kemiska Institutionen, Uppsala, Sweden, Private Communication, 1991.
(15) Busch, G.; Vogt, O. *Helv. Phys. Acta* **1976**, *33*, 437.
(16) Schmid, M.; Mooser, P. H. E. *Phys. Rev.* **1975**, B12.
(17) Chalbtov, V. K. *An Introduction to Semiconductor*; 1969. (In Russian).
(18) Schluter, M. *Nuovo Cimento B* **1973**, *13*, 313.
(19) Belenkil, G. I.; Stopachinshii, V. B. *USP Fiz. Nauk* **1983**, *140*, 233.
(20) Bube, R. *Photoconductivity of solids*; Wiley: New York, 1960.
(21) Bardeen, J.; Shockley, W. *Phys. Rev.* **1950**, *80*, 72.
(22) Nagat, A. T. *J. Condens. Matter* **1989**, *1*, 7921−7924.
(23) Pan, D. S.; Lu, Y.; Chu, M. *Appl. Phys. Lett.* **1988**, *53*, 307.
(24) Tagirov, V. I.; Gakhramanov, N. F.; Guseinov, A. G.; Aliev, F. M. *Sov. Phys. − Semicond.* **1983**, *17*, 32.
(25) Morin, F. J.; Maita, J. P. *Phys. Rev.* **1954**, *94*, 1525.
(26) Rose, A. *Concepts in Photoconductivity*; Wiley-Interscience: New York, 1963.